ENHANCING RETINAL VESSEL SEGMENTATION BY COLOR FUSION

Xiaohong Wang , Xudong Jiang

School of Electrical & Electronics Engineering
Nanyang Technological University, Singapore 639798

ABSTRACT

Accurate segmentation of retinal vessel plays an important role in the computer-aided diagnosis of eye diseases. Existing supervised methods extract features only from green channel due to its much higher contrast between vessel and background than in red and blue channels. However, red and blue channels also contain useful information for distinguishing vessel from background. This work investigates various ways of combining information in all 3 color channels to enhance the segmentation performance, based on which an effective color fusion scheme is proposed in this paper. Its performance is evaluated on two publicly available databases DRIVE and STARE. Results demonstrate that the proposed feature fusion with dimensionality reduction by asymmetric PCA visibly enhances the segmentation performance consistently on both databases, rendering better performance than state-of-the-art methods in dealing with healthy and pathological retinal images.

Index Terms— Retinal vessel segmentation, color fusion, dimensionality reduction.

1. INTRODUCTION

Retinal vessel segmentation from digital fundus images is a crucial step required for computer-aided medical image analysis, especially for the diagnosis of some ophthalmic pathologies, such as diabetic retinopathy and age-related macular degeneration [1]. However, due to the low contrast between retinal vessel and background, the pathological effects of the retinal diseases, and the variations in vessel diameters, accurate retinal vessel segmentation is still a great challenging task. Many approaches have been reported to address these problems, which can be divided into two groups: unsupervised methods [2-7] and supervised methods [8-14].

The unsupervised methods are mainly rule-based, like matched filter (MF) [2, 3], vessel tracking [4, 5] and deformable models [6, 7]. Those methods implement retinal vessel segmentation without considering the information of ground truths. For example, vessel tracking method tracks vessels based on their local patterns [4]. Deformable model focuses on capturing the shape of the retinal vessel by an iterative adaption [6].

The supervised methods classify each image pixel into vessel or background by training some classifiers. Staal *et al*. [8] implement vessel classification by using a KNN classifier with sequential forward feature selection. In [9], feature vector is composed of the pixel intensity and 2-D Gabor wavelet transformation response, and a Bayesian classifier with Gaussian mixture model (GMM) is applied for classification. You *et al*. [10] classify the feature vector derived from the steerable complex wavelet by SVM classifier. Marin *et al*. [11] construct a 7-D feature vector consisting of the moment-invariant and gray-level information, followed by classification with a five-layer feed-forward neural network. Fraz *et al*. [12] compute a 9-D feature vector for vessel pixel classification with an ensemble classifier of the boosted and bagged decision trees. Vega *et al*. [13] use a lattice neural network with dendritic processing (LNNDP) to classify feature vector. Fu *et al*. [14] utilize a fully convolutional neural networks (CNNs) to generate a vessel probability map.

Although approaches mentioned above exhibit good ability for retinal vessel segmentation, several aspects still need to be improved, such as loss of thin vessels and false detection of non-vessel structures. Existing supervised methods extract features only from green channel, as this channel provides the highest contrast between retinal vessel and background. In fact, other color channels also contain useful information for retinal image analysis. For example, optic disc is often brighter in red channel, along with a well-defined white shape [15], leading to a distinguishable feature for optic disc representation. In order to extract the information that is difficult to be detected in green channel, this paper investigates four different color fusion methods and proposes to build a robust feature space based on the feature fusion with dimensionality reduction. To the best of our knowledge, this is the first work that fuses color information to classify retinal vessel. Besides, we utilize a two-step postprocessing procedure to further improve the vessel detection rate.

The contributions of this paper are: (1) investigate four different ways of fusing color information and based on that propose the most effective fusion scheme, (2) improve classification accuracy by using a two-step postprocessing procedure, and (3) achieve the state-of-the-art performance on two evaluated databases.

2. PROPOSED VESSEL SEGMENTATION METHOD

2.1. Feature extraction

The feature vector contains quantifiable measures for classifier to decide a candidate pixel as retinal vessel or background. For each pixel, we construct a 118-D feature vector, encoding information on spatial property and local intensity distribution in 3 color channels. Many features have been widely used for vessel representation, like Gabor transformation [9] and line strength [12]. Besides of these well-known features, we also propose to use other features reported on the field of retial image analysis, e.g. the first derivative of each matched filter [2], Frangi filter at multiple scales [16] and equalized illumination features [17]. Each component of the feature vector is described as follows.

(1) *Matched filter (eight features per scale, total 32 features)*: Considering that the cross-section of retinal vessel can be modeled by a Gaussian shaped curve [2], we extract features by convolving retinal images with a set of 2D Gaussian kernels at four scales (σ=[1,2,3,4]) and four length (L=[5,7,9,11]). To detect retinal vessel boundary, we design another feature, i.e. the convolution of the retinal image and the first derivative of each Gaussian kernel. This feature for a pixel belonging to edge is non-zero, making boundary between vessel and background distinguishable.

(2) *Frangi filter (four features per scale, total 16 features)*: Frangi filter [16] is a process that detects the tubular shape in retinal images based on eigenvalue analysis of the Hessian matrix. To better delineate retinal vessel geometrical structure, we take one vesselness measure, one Frobenius norm and two principal curvatures at four scales as features.

(3) *Equalized illumination features (four features)*: This feature results from an enhanced retinal map where the effect of illumination is equalized [17]. We increase the contrast of image and suppress the noise amplification by changing the local window size for histogram equalization from 4 to 10 at increment of 2.

Other features can be briefly expressed as: (4) 2-D Gabor wavelet transformation (five features) [9]; (5) Line strength (four descriptors per length, total 28 features) [12]; (6) Moment invariant-based features (two measures per window size, total 14 features) [11]; (7) Two ridge measures based on the derivatives of Gaussian kernels at four scales (two measures per scale, eight features) [18]; (8) Morphological top-hat transformation using structure elements with different radius (five features) [12]; (9) Difference of Gaussian at three scales (three features); (10) Features based on discontinuities in gradient orientation (three features) [12].

2.2. Color fusion

Rather than merely using green channel as the previous research, we investigate four color fusion methods based on different fusion processing levels, as shown in Figs. 1-4. Although neural classifiers [19] may achieve higher accuracy, much effort is required in parameter tuning. This work investigates the effect of color fusion and hence the same SVM classifier [20] is used in all fusion schemes. Let $I_r(x,y)$, $I_g(x,y)$ and $I_b(x,y)$ be the input intensity of image in red, green and blue channels, whose corresponding feature vector is $\mathbf{f}_r(x,y)$, $\mathbf{f}_g(x,y)$ and $\mathbf{f}_b(x,y)$, respectively. The size of each feature vector is M which equals to 118 in this work.

(1) *Pixel intensity fusion* (PIF): This is the simplest fusion that combines the information at the earliest stage, i.e. $I_p = [w_r\, w_g\, w_b][I_r\, I_g\, I_b]^T$. The same feature extraction and classification as those used in a single color channel is applied in the combined intensity channel. Two common PIF methods are fusions from RGB color channels to grayscale channel (PIF_g) and luminance channel (PIF_l), where $[w_r\, w_g\, w_b]$ is [0.299 0.587 0.114] and [0.209 0.715 0.0076], respectively. Both pixel intensity fusion methods assign higher weights to the green channel. Clearly, fusions at pixel intensity level are easy to be implemented, but they ignore vessel spatial structure in each individual color channel, thus cannot consistently improve the segmentation performance, as shown in the experiment later.

Fig. 1. Diagram of pixel intensity fusion.

(2) *Decision fusion* (DF): At the last stage, fusion is the process of merging binary classification results which derive from SVM classifiers on three color channels. The relationship between binary classification result and feature vector $\mathbf{f}$ is defined by [20]

$$D(\mathbf{f}) = \text{sign}(\sum_{k=1}^{n} a_k y_k G\left(\mathbf{f}^k, \mathbf{f}\right) + b), \qquad (1)$$

where a_k and b are the estimated parameters. $\mathbf{f}^k$ is the k-th support vector whose corresponding class label is y_k. An exponential kernel G is applied in this paper to map data into the hyperplane. The binary classification results provided by SVM are then fused using a majority voting method. Though fusion at the decision level preserves vessel spatial information in each individual channel, it ignores the quantitative difference among different channels.

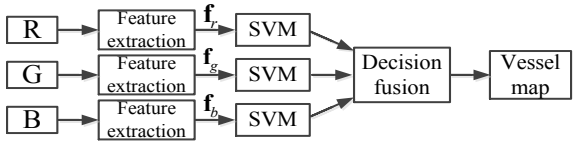

Fig. 2. Diagram of decision fusion.

(3) *Score fusion* (SF): Different from decision fusion that uses only the binary classification results, score fusion incorporates the classification confidence level that quantifies the reliability of a pixel classified as vessel or background. The function of classification score is expressed by

$$S(\mathbf{f}) = \sum_{k=1}^{n} a_k y_k G\left(\mathbf{f}^k, \mathbf{f}\right) + b, \tag{2}$$

where S is the similarity score of the input $\mathbf{f}$ to the classes. In this paper, score fusion is achieved by aggregating S with SVM classifier. The fusion at the score level takes into account different each color channel quantitatively, but it ignores the correlation information among features extracted in different color channels.

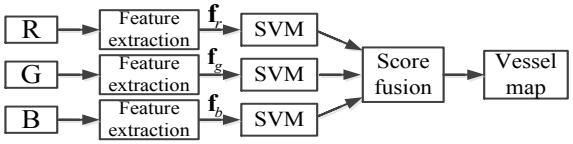

Fig. 3. Diagram of score fusion.

(4) *Feature fusion with dimensionality reduction* (FF_{dr}): To use the complete information in the fusion process, features from RGB color channels are concatenated to form a new feature vector $\mathbf{f}' = [\mathbf{f}_r\, \mathbf{f}_g\, \mathbf{f}_b]$. Obviously, this concatenation process creates a high-dimensional feature vector, i.e. 354, three times more than that in the single color channel. Nevertheless, techniques of dimensionality reduction can be applied to solve the curse of dimensionality. Principal component analysis (PCA) is a fundamental tool of dimensionality reduction by removing the unreliable dimensions caused by unrepresentative training data [21]. However, the numbers of positive class (retinal vessels) and negative class (background) are highly asymmetric, e.g. only 10.4% of pixels are marked as vessels on STARE database. PCA does not effectively work on this unbalance data because it puts a larger eigenvalue bias on the negative class. To tackle this problem, a covariance mixture of asymmetric PCA [22] is constructed:

$$\Sigma_t = \gamma\Sigma_v + (1-\gamma)\Sigma_b + \Sigma_m, \tag{3}$$

where Σ_v, Σ_b and Σ_m are the covariance matrices of vessel class, background class and the covariance matrix of the two class means (also called the between class scatter matrix), respectively. γ is a weighting factor to balance the two classes. If $\gamma = N_v/(N_v + N_b)$ where N_v and N_b are the numbers of retinal vessel and background pixels, respectively, Σ_t is the same as total scatter matrix used in PCA. Here, we assign a high weight ($\gamma = 0.5$, compared with $\gamma \approx 0.1$ for PCA) to Σ_v so that the effect of the two unbalanced classes is reduced.

Eigen-decomposition on covariance mixture is performed, $\Sigma_t = \Phi\Lambda\Phi^T$, where Φ and Λ denote the eigenvectors and eigenvalues of Σ_t, respectively. Asymmetric PCA (APCA) takes eigenvectors corresponding to the largest eigenvalues to project feature vector $\mathbf{f}$ to a subspace. This work uses APCA [22] to reduce the fussed feature dimensionality from 354 to 118, the same as that of a single color channel.

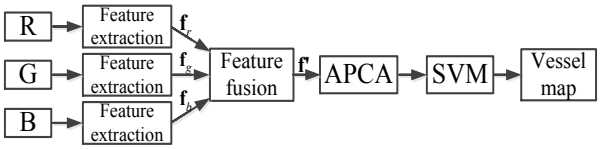

Fig. 4. Diagram of feature fusion.

2.3. Postprocessing

Misclassification exists in some special locations, e.g. lesions with variation shapes, isolated points in wide vessels and background. In this paper, a two-step postprocessing operation is proposed by analyzing the property of corresponding regions. Firstly, the segmented vessel map is skeletonized, followed by region growing to smooth the edge of the detected vessels. Secondly, isolated points misclassified as vessels in background are removed while small holes completely surrounded by wide vessels are filled.

3. EXPERIMENTS

The proposed method is tested on two publicly available databases: DRIVE [8] and STARE [23]. Table 1 illustrates the performance comparison of the 3 color channels and various color fusion schemes. It is not a surprise that the green channel has much higher accuracy than the 2 other channels. The two simple color fusion schemes, pixel intensity fusion and decision fusion, fail to deliver better performance than the best single channel consistently over the two databases. Although the score fusion delivers better performance than the best single channel consistently, the improvement is very marginal. Table 1 shows that the proposed feature fusion with dimensionality reduction outperforms all other approaches visibly and consistently over the two databases.

Table 1. Performance comparison of color fusion methods on DRIVE and STARE databases.

	DRIVE		STARE	
	Accuracy	Sensitivity	Accuracy	Sensitivity
RED	93.39%	55.03%	93.27%	42.99%
GREEN	94.85%	67.64%	96.02%	70.85%
BLUE	93.36%	56.38%	90.70%	18.56%
PIF_g	94.95%	68.40%	95.70%	67.61%
PIF_l	94.95%	68.46%	95.85%	69.00%
DF	94.33%	61.78%	94.14%	46.52%
SF	94.91%	68.23%	96.03%	70.99%
FF_{dr}	**95.11%**	**73.15%**	**96.20%**	**75.91%**

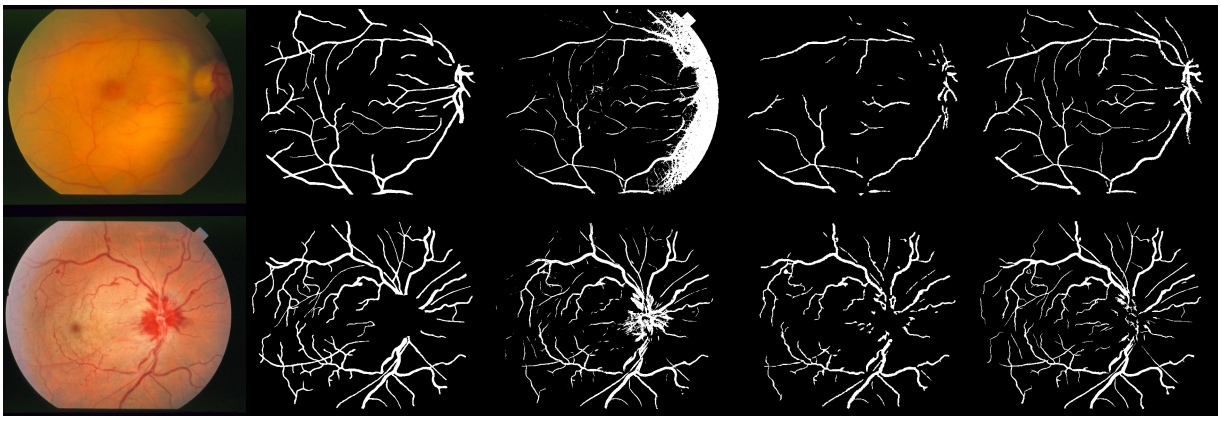

Fig. 5. Segmentation results of pathological images. First to last column: original pathological image, ground truth, results from Soares *et al.* [9], Marin *et al.* [11] and the proposed method.

Table 2 illustrates the performance comparison with state-of-the-art methods on two databases, where the proposed method achieves the best accuracy and sensitivity. For DRIVE and STARE databases, the proposed method improves segmentation performance (accuracy, sensitivity) from (94.80% [12], 74.44% [13]) to (95.19%, 74.79%), and from (95.45% [14], 75.48% [12]) to (96.27%, 78.44%), respectively.

Table 2. Performance comparison with state-of-the-art methods on DRIVE and STARE databases.

Method	Year	DRIVE		STARE	
		Accuracy	Sensitivity	Accuracy	Sensitivity
Hoover [23]	2000	N.A	N.A	92.64%	67.47%
Jiang [1]	2002	92.12%	N.A	90.09%	N.A
Staal [8]	2004	94.41%	N.A	95.16%	N.A
Soares [9]	2006	94.61%	73.32%	94.79%	72.07%
Marin [11]	2011	94.52%	70.67%	95.26%	69.44%
You [10]	2011	94.34%	74.10%	94.97%	72.60%
Fraz [12]	2012	94.80%	74.06%	95.34%	75.48%
Vega [13]	2015	94.12%	74.44%	94.83%	70.19%
Fu [14]	2016	94.70%	72.94%	95.45%	71.40%
FF_{dr}	2016	95.11%	73.15%	96.20%	75.91%
$FF_{dr}{}^*$	2016	**95.19%**	**74.79%**	**96.27%**	**78.44%**

$FF_{dr}{}^*$: Proposed method with postprocessing.

The STARE database contains ten images with abnormality, like background diabetic retinopathy and central retinal artery/vein occlusion. Classification performance (accuracy, sensitivity) in different literatures for those pathological images are listed in Table 3. Clearly, the proposed method performs better than others in handling pathological images, e.g. producing about (0.89% [11], 3.45% [12]) improvement for each measurement.

Fig. 5 shows segmentation results of two pathological retinal images based on methods in [9], [11] and the proposed method. Method in [9] segments more non-vessel pixels, especially some pathological regions like the red lesions in second row, while method in [11] loses some structures of retinal vessels, such as thin vessels that connect with vessel trees. Comparatively, the proposed method can detect vessel and background pixels more accurately, showing better performance on segmentation of pathological images.

Table 3. Performance comparison on STARE pathological images.

Method	Hoover [23]	Soares [9]	Marin [11]	Fraz [12]	FF_{dr}	$FF_{dr}{}^*$
Sensitivity	65.87%	71.81%	62.23%	72.62%	71.91%	**76.07%**
Accuracy	92.58%	95.00%	95.22%	95.11%	96.02%	**96.11%**

$FF_{dr}{}^*$: Proposed method with postprocessing.

4. CONCLUSION

This work investigates various ways of color fusion to enhance the segmentation performance of retinal vessels, based on which an effective fusion scheme is proposed in this paper. The simple color fusion in the earliest stage at pixel intensity level ignores vessel spatial structure in individual color channel and hence cannot consistently improve the segmentation performance. Similarly, the simple color fusion in the last stage at decision level ignores the quantitative difference among different color channels and hence performs undesirably. The fusion at the classification score level performs better than the best single channel consistently on the two databases. However, the performance improvement is very marginal since it ignores the correlation among features extracted in different color channels. The proposed color fusion at feature level with dimensionality reduction by asymmetric PCA shows visible performance enhancement consistently on both databases, rendering better performance than state-of-the-art methods. Moreover, the proposed method also performs well for pathological images with different lesions, making it useful for computer aided screening for patients with eye diseases.

5. REFERENCES

[1] X. Jiang and D. Mojon, "Adaptive local thresholding by verification-based multithreshold probing with application to vessel detection in retinal images," *IEEE Trans. Pattern Anal. Mach. Intell.*, vol. 25, no. 1, pp. 131–137, 2003.

[2] S. Chaudhuri, S. Chatterjee, N. Katz, M. Nelson, and M. Goldbaum, "Detection of blood vessels in retinal images using two-dimensional matched filters," *IEEE Trans. Med. Imag.*, vol. 8, no. 3, pp. 263–269, 1989.

[3] M. M. Fraz, S. A. Barman, P. Remagnino, A. Hoppe, B.and Rudnicka A. R. Basit, A.and Uyyanonvara, and C. G. Owen, "An approach to localize the retinal blood vessels using bit planes and centerline detection," *Comput. Methods Programs Biomed.*, vol. 108, no. 2, pp. 600–616, 2012.

[4] A. Can, H. Shen, J. N. Turner, H. L. Tanenbaum, and B. Roysam, "Rapid automated tracing and feature extraction from retinal fundus images using direct exploratory algorithms," *IEEE Trans. Inform. Technol. Biomed.*, vol. 3, no. 2, pp. 125–138, 1999.

[5] Y. Yin, M. Adel, and S. Bourennane, "Retinal vessel segmentation using a probabilistic tracking method," *Pattern Recognit.*, vol. 45, no. 4, pp. 1235–1244, 2012.

[6] T. McInerney and D. Terzopoulos, "T-snakes: Topology adaptive snakes," *Med. Image Anal.*, vol. 4, no. 2, pp. 73–91, 2000.

[7] Y. Q. Zhao, X. H. Wang, X. F. Wang, and F. Y. Shih, "Retinal vessels segmentation based on level set and region growing," *Pattern Recognit.*, vol. 47, no. 7, pp. 2437–2446, 2014.

[8] J. Staal, M. D. Abràmoff, M. Niemeijer, M. Viergever, and B. Van Ginneken, "Ridge-based vessel segmentation in color images of the retina," *IEEE Trans. Med. Imag.*, vol. 23, no. 4, pp. 501–509, 2004.

[9] J. V. Soares, J. J. Leandro, R. M. Cesar Jr, H. F. Jelinek, and M. J. Cree, "Retinal vessel segmentation using the 2-d gabor wavelet and supervised classification," *IEEE Trans. Med. Imag.*, vol. 25, no. 9, pp. 1214–1222, 2006.

[10] X. You, Q. Peng, Y. Yuan, Y. M. Cheung, and J. Lei, "Segmentation of retinal blood vessels using the radial projection and semi-supervised approach," *Pattern Recognit.*, vol. 44, no. 10, pp. 2314–2324, 2011.

[11] D. Marín, A. Aquino, M. E. Gegúndez-Arias, and J. M. Bravo, "A new supervised method for blood vessel segmentation in retinal images by using gray-level and moment invariants-based features," *IEEE Trans. Med. Imag.*, vol. 30, no. 1, pp. 146–158, 2011.

[12] M. M. Fraz, P. Remagnino, A. Hoppe, B. Uyyanonvara, A. R. Rudnicka, C. G. Owen, and S. Barman, "An ensemble classification-based approach applied to retinal blood vessel segmentation," *IEEE Trans. Biomed. Eng.*, vol. 59, no. 9, pp. 2538–2548, 2012.

[13] R. Vega, G. Sanchez-Ante, H. Falcon-Morales, L. E.and Sossa, and E. Guevara, "Retinal vessel extraction using lattice neural networks with dendritic processing," *Comput. Biol. Med.*, vol. 58, pp. 20–30, 2015.

[14] H. Fu, Y. Xu, D. Wong, and J. Liu, "Retinal vessel segmentation via deep learning network and fully-connected conditional random fields," in *Proc. IEEE Conf. International Symposium on Biomedical Imaging*, 2016, pp. 698–701.

[15] A. Aquino, M. E. Gegúndez-Arias, and D. Marín, "Detecting the optic disc boundary in digital fundus images using morphological, edge detection, and feature extraction techniques," *IEEE Trans. Med. Imag.*, vol. 29, no. 11, pp. 1860–1869, 2010.

[16] A. F. Frangi, W. J. Niessen, K. L. Vincken, and M. A. Viergever, "Multiscale vessel enhancement filtering," in *Proc. 1st MICCAI*, 1998, pp. 130–137.

[17] A. Salazar-Gonzalez, D. Kaba, Y. Li, and X. Liu, "Segmentation of the blood vessels and optic disk in retinal images," *IEEE J. Biomed. Health Inform.*, vol. 18, no. 6, pp. 1874–1886, 2014.

[18] T. Lindeberg, "Edge detection and ridge detection with automatic scale selection," *Int. J. Comput. Vision*, vol. 30, no. 2, pp. 117–156, 1998.

[19] X. D. Jiang and A. H. K. S. Wah, "Constructing and training feed-forward neural networks for pattern classification," *Pattern recognition*, vol. 36, no. 4, pp. 853–867, 2003.

[20] S. Abe, *Support vector machines for pattern classification*, vol. 53, Springer, 2005.

[21] X. D. Jiang, "Linear subspace learning-based dimensionality reduction," *IEEE Signal Process. Mag.*, vol. 28, no. 2, pp. 16–26, 2011.

[22] X. D. Jiang, "Asymmetric principal component and discriminant analyses for pattern classification," *IEEE Trans. Pattern Anal. Mach. Intell.*, vol. 31, no. 5, pp. 931–937, 2009.

[23] A. Hoover, V. Kouznetsova, and M. Goldbaum, "Locating blood vessels in retinal images by piecewise threshold probing of a matched filter response," *IEEE Trans. Med. Imag.*, vol. 19, no. 3, pp. 203–210, 2000.